

Measurement and Characterisation of Fractures in Parts of the Togo Structural Units (TSU) and Dahomeyan Gneissic Complex (DGC), SE Ghana

Amadu Casmed Charles*

Earth and Environmental Sciences Department, University for Development Studies (UDS)
P. O. Box 20, Navrongo, Ghana

Gawu Simon K.Y. and Appiah-Agyei Emmanuel
Department of Geological Engineering

Kwame Nkrumah University of Science and Technology (KNUST), Kumasi, Ghana

Abstract

Fracture characterisation in fractured rocks is a critical step in the generation of discrete fracture network (DFN) modelling and the evaluation of the hydraulic and mechanical properties of the rockmass. In this study, an integrated approach of using structural geological mapping, linear and circular scanline mappings, and laboratory investigation of rock samples were undertaken at two selected sites, Site 1, within the Togo structural units (TSU) near Ablekuma settlement, and Site 2 within the Dahomeyan Gneissic Complex (DGC), near Danfa settlement to derive information on fracture characteristics in the Study Area. A total of 1128 fractures were surveyed along a total length of 238 m of scanline at Site 1, and 629 fractures along a total of 156.0 m at Site 2. Fourteen and thirteen circular scanlines were surveyed at Site 1 and Site 2 respectively. Linear fracture density or intensity (P_{10}) from the 7 scanlines at Site 1 ranged from 3.50 fractures/m to 6.26 fractures/m, compared to fractures at Site 2, which have fracture linear density ranging from 2.34 fractures/m to 5.04 fractures/m. The mean linear fracture intensity for Site 1 was computed as 4.739 fractures/m from 1128 fractures along 238.0 m scanline length, and 4.030 fractures/m from 629 fractures along a total of scanline of 156.0 m for Site 2. The DIPS software was used to analyse the orientation data, while the EasyFit used for modelling fracture spacing distribution. The best fit model for fracture spacing at Site 1 was a negative 2-parameter exponential distribution function (pdf), while that for Site 2 was a negative exponential distribution. There appear to be a lithological and/or stratigraphic thickness control on fracture density, as fracturing was more intense in the medium grained less thick quartzite beds of the Site 1, within TSU compared to the coarse grain much thicker stratigraphic units of gneiss of Site 2 within the DF.

Keywords: Fracture characterisation, Togo Structural Units, Dahomeyan Gneissic Complex.

1.0 Introduction

Fractures and other mechanical discontinuities are prevalent in natural and synthetic structural media, even in some of the best engineered materials. Fractures often occur as a set of discontinuities, and are known to be pervasive in the Earth's upper crust (Leary et al., 1990). They range in size from micro-cracks to faults and lineaments. The term 'fracture' can be defined in diverse ways, depending on the focus of the study (Van der Pluijm and Marshak, 2004). In this study, a fracture is defined as, an approximately planar discontinuity, such as joint, foliation plane, fault, dyke, or vein (Peacock et al., 2000).

Rock fracture networks and their geometric characteristics are the most effective factors on rock permeability (Brace 1980; Brown 1989), deformability, strength and stability (Goodman 1976; Brown and Scholz 1986; Hudson and Harrison, 1997). Fractures play significant roles in fluid flow in rockmasses, and constitute one of the prominent investigations in hydrogeology, civil works, mining and the disposal of waste. Information on fracture characteristics such as orientation, spacing and trace length are used in generating stochastic models of fracture networks (San, 2009). In recent years stochastic models are developed for the purpose of investigating the effects of aperture of the fractures on hydro-mechanical and mechanical behaviour of fractured rockmass.

Some of the approaches often adopted to characterise fractures and fracture networks in the subsurface include, borehole drilling and logging, outcrop linear and window mapping, and fluid-flow experiments (Boadu and Long, 1996). Borehole cores and image logs provide valuable in-situ information on, for example, fracture spacing, orientation, aperture, and cementation (Olson et al., 2009), however, fracture sampling from borehole cores are strongly affected by borehole inclination. Fracture intersection frequency is highest for a borehole perpendicular to the set fractures, whereas if the borehole is parallel to the fracture set, sampling is very limited, and no, or only few data can be acquired. Borehole drilling and fluid-flow experiments are expensive in their operation, and probably beyond the budgets of most local authorities and individuals. A relatively inexpensive way to characterise a fractured medium is the use of linear scanline (Einstein and Baecher, 1983; Priest 1993),

and window mapping (Pahl, 1981; Priest, 1993; Mauldon et al., 2001; Rohrbaugh et al., 2002), particular where there are rock exposures and outcrops. Furthermore, measuring on rock exposure has the advantage of using a vast area for surveying geometric properties such as orientation, persistence and other large scale geometric features. Geological relationships between the groups of the fractures is also observable in the rock exposure.

Biases resulting from drillhole orientation can be minimised in the case of outcrop

linear scanline sampling, since the scanlines are oriented to intercept the dominant fracture sets at close to normal as possible. The method allows a lot of fracture attribute data to be collected much quicker compared to drilling. It does not also require new invasion of ground. Also, the circular scanline method, outlined by Mauldon (1998), Mauldon et al. (2001) and Rohrbaugh et al. (2002), can be used to estimate fracture density and intensity, and mean trace length of fractures at a study site.

The main objective of this study is to, characterise the fractures in parts of the TSU and the DF in south-eastern Ghana, based on fracture surveys from outcrops and rock exposure.

2.0 Study area

The study area is located administratively within the Greater Accra Metropolitan Area (GAMA) in the Greater Accra Region of Ghana. It is one the fastest urbanising regions in the country. For the purpose of this research, the study area shall be referred to as the Accra-Tema area (ATA). It extends from Weija in the southwest to Danfa in the northeast. It is located between latitudes $5^{\circ} 30' 0''$ N and $5^{\circ} 49' 0''$, and longitudes $0^{\circ} 8' 00''$ W and $0^{\circ} 20' 00''$ W, with a total land area of about 700 sq. km (Figure 1).

ATA lies within the coastal savannah zone, which is the driest climatic zone in Ghana (Dickson and Benneh; 1988; Muff and Efa, 2006). The zone exhibits a double maxima rainfall regime with an annual rainfall of between 1145 and 1650 mm. The major and minor rainy seasons are respectively from April to July, and September to November, while from December to February is dry with high temperatures (Anon. 1997). The highest average monthly temperatures (mean 28.4°C) occur during February, whilst the lowest (mean 25.1°C) in August. Average relative humidity varies between 65% in the dry season to about 95% in the rainy season (Anon (1997; Muff and Efa, 2006). The vegetation is the coastal savannah grassland, characterised by short savannah grass interspersed with shrubs, short trees and small thickets along streams and mangroves (Dickson and Benneh, 1980).

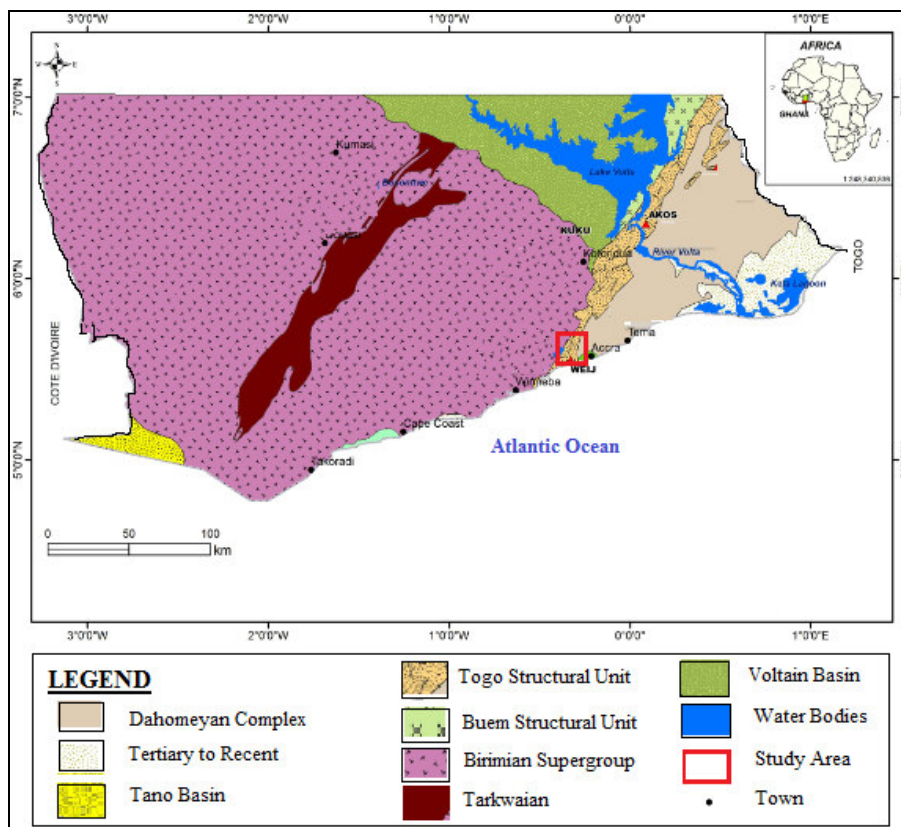


Figure 1 Geological map of southern Ghana showing location of study area (edged red) (Modified after GSD, 1988).

The geology of study area has been studied extensively by several workers (e.g. Junner, 1940; Bates, 1946; Hirst, 1948; Mason, 1957; Harris, 1970; Ahmed et al., 1977; Mani, 1978; Blay, 1982; Kesse, 1985; Muff and Efa,

2006). On the basis of age, tectonic evidence, lithologic characteristics, metamorphism and field relations, four major lithologic units can be distinguished in the study area (Kesse, 1995; Amponsah et al 2012; Akpan et al., 2016) (Figure. 2), namely, the Accraian, the Togo Structural units (TSU), the Dahomeyan, and the Cape Coast Granitoid Complex (Eburnean basin type granitoid intrusive).

Rocks of the STU and DF cover about 90% of the total study area, TSU making up 50 % and DF making up 40 %. Table 1 is a summary of the stratigraphic succession and the main lithological units.

Table 1 Stratigraphic succession of the main lithological units of ATA (Modified after Junner, 1932)

Division	Lithologies
Unconsolidated and poorly consolidated rocks (quaternary or tertiary age)	Sediments and superficial deposits: Marine, fluvial or lagoonal sediments, alluvium, terrace gravels, soils, colluvium, and lateritic clays
Accraian (Mid-Devonian)	Sandstone, grit and shale
Togo Structural Unit (Upper Precambrian)	Quartzite, sandstone, shale, phyllite, schist and silicified limestone. check
Thrust contact	
Dahomeyan (Upper Precambrian)	Acidic, ortho- and paragneiss and schist and migmatite, many of which are rich in garnet, hornblende and biotite.
Cape Coast Granite Complex (Mid-Precambrian)	Granitoid undifferentiated.

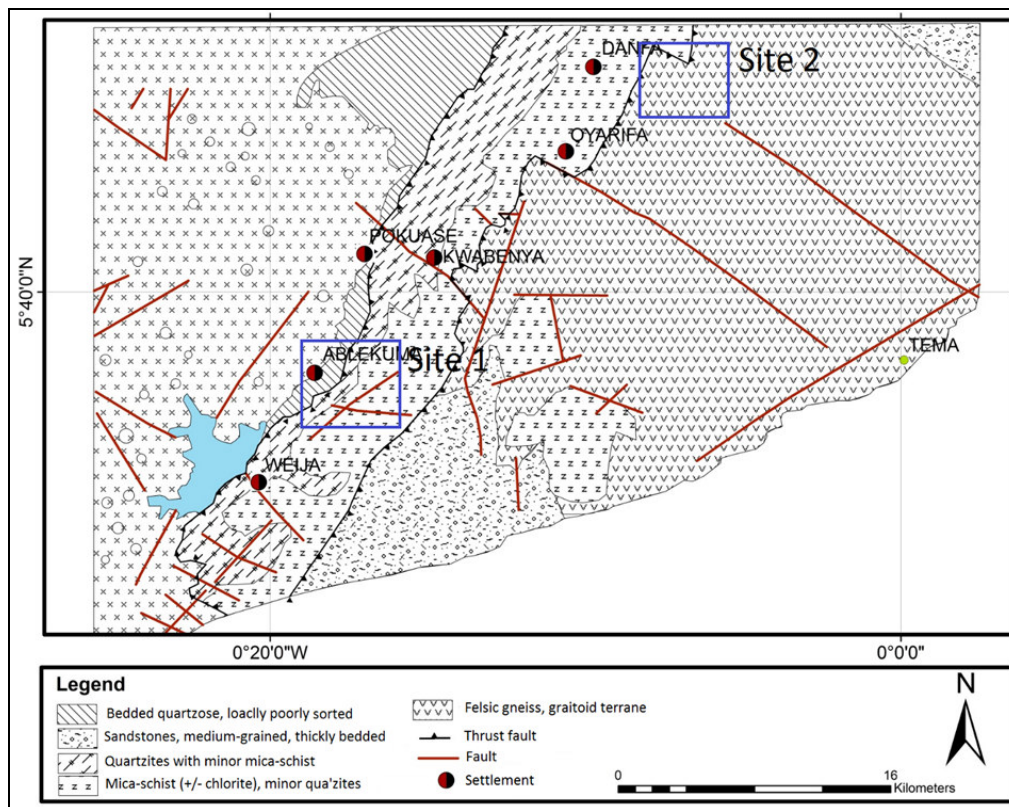


Figure. 2 Sketch Map of part of Southern Ghana showing location of Study Sites (Modified from Muff and Efa, 2006). Site 1 is near Ablekuma settlement within the STU, and Site 2 is near Danfa, within Dahomeyan formation.

3.0 Materials and Methods

3.1 Field Work

3.1.1 Geological and Structural Mapping, and Interpretation of Structural Data of the Study Area

Fieldwork was carried out between July and November, 2015. A reconnaissance survey was first carried out, which involved identifying and locating outcrops and rock exposures large enough for fracture sampling within the TSU and DGC.

The initial surface geological study involved mapping of geological structures of rock exposures and

collection of rock samples at selected locations for thin section preparation. Structural mapping was carried out along north-south traverse. Traversing crossing strikes or trends of major rock units, with the aid of topographic maps sheets obtained from the Ghana Geological Survey Department. Structures observed and recorded at district-scale were foliations, faults and in few occasions lithological contacts. Figure 3 are photographs of examples of the studied rock exposures within the study area. Preliminary mineral assemblages and micro-structural observation from hand lens observations were also recorded

Lower-hemisphere equal-area projections of structural data for the different rock formations (TSU and DGC) and lithological units were generated for interpretation.

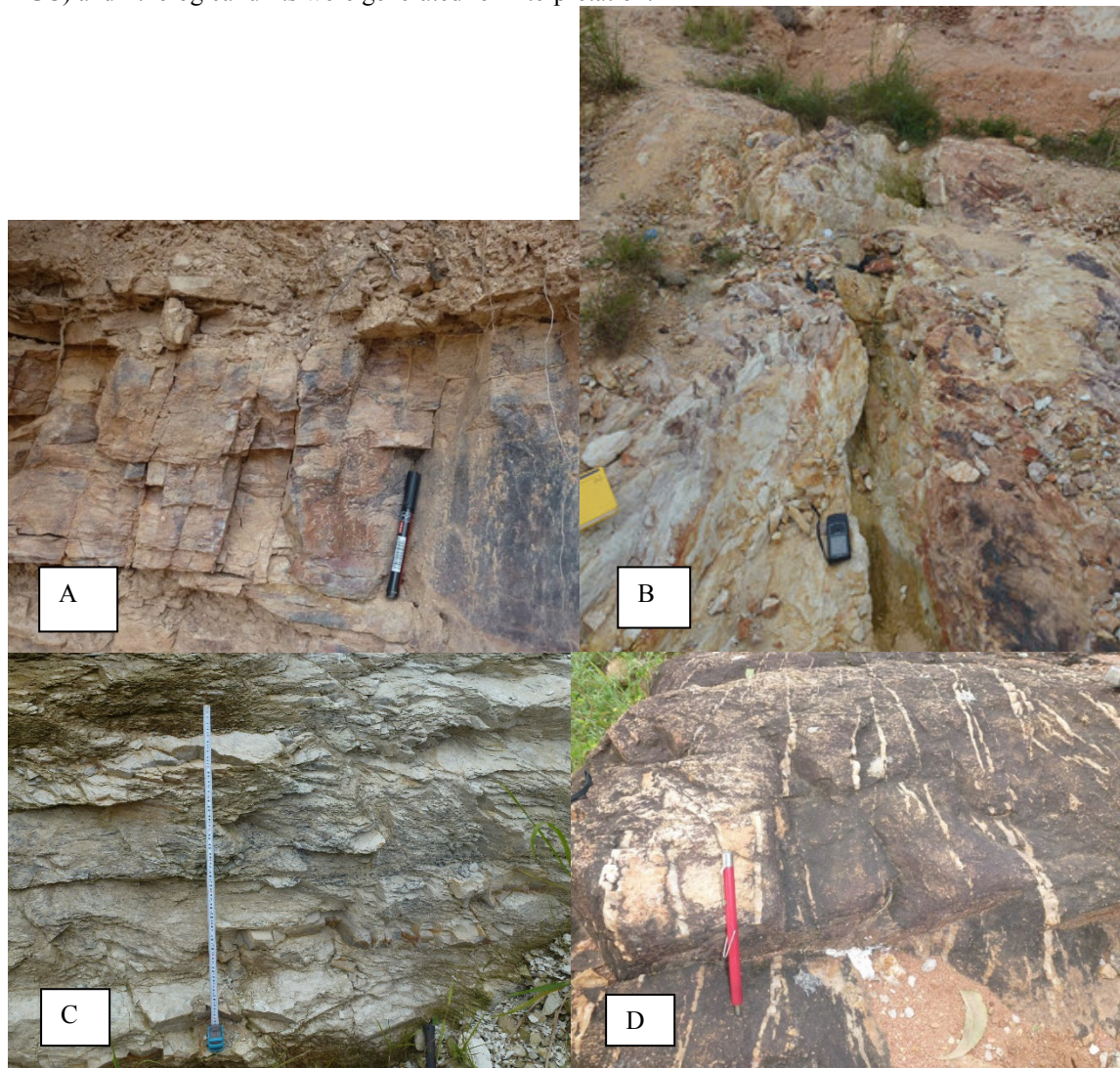


Figure 3 Photographs of Examples of Structures Observed in the Study Area. (A) Jointed Rock Mass, Site 1 (Ablekuma area), (B) Major Fault in Quartzite (Ablekuma area), (C) Schist, Politic Composition, Schistose Textured (Ablekuma area), (D) Highly Silicified Gneiss with Quartz Veining, Site 2 (Danfa area)

3.1.2 Fracture Data Collection

Linear Scanline Mapping

1128 fractures from seven (7) linear scanlines, along a total of 238.0 m were surveyed at Site 1, and 629 fractures along a total of 156.0 m were surveyed from four (4) scanlines at Site 2. Prior to measurements of fracture attributes, the exposed rock mass was described (rock type, colour, grain size, degree of weathering, etc.) with the aid of a hand lens. For each fracture, the following attributes were recorded: fracture type (foliation, joint, fault, vein, etc.), orientation or attitude, distance from the start point of scanline, fracture trace length, fracture aperture, and infill material.

Measurements of trace length and aperture were recorded in a field notebook and subsequently entered into a Microsoft Excel spreadsheet. Station locations were stored as waypoints in the memory of the GPS device and subsequently transferred to an Excel spreadsheet via a USB data connection to a PC.

The length of scanlines were varied from 20–48 m depending on the amount of continuous exposure,

changes in lithology and structure.

3.2 Fracture Data Analysis

3.2.1 Orientation and Identification of Fracture Sets

Fractures are assumed to be planar (Hudson and Harrison, 1997) and so, the dip angle, strike, and the dip direction uniquely define the orientation of the fracture. To identify fracture sets, dips and dip directions values recorded from linear scanlines were, imported into DIPS (Rocscience Inc., 2012). The orientation of each fracture plane was plotted in a stereographic projection. The measured attitude values were sorted for the various rock types in each study site and analysed separately. They were also treated as combined data. Plots of poles provided a visual depiction of pole concentrations. By contouring the pole plots, the most highly concentrated areas of poles, representing the dominant fracture sets were identified.

Linear Intensity and Density

Linear Intensity is obtained by dividing the number of fractures (N) by the total length (L) of the scanline:

$$F_1 = \frac{N}{L} \quad (4.3)$$

This expression is the same as linear fracture density (d_1 or P_{10}), which is defined as, the average number of fractures per unit length. It equals fracture frequency (F_f), and is the reciprocal of fracture spacing.

The linear fracture intensity (P_{10}) for Site 1 was computed as 4.739 fractures/m from 1128 fractures along 238.0 m scanline length, and 4.030 fractures/m from 629 fractures along a total of scanline of 156.0 m for Site 2.

Fractures Mean Trace Length and Areal Density

The size of fractures is an important but difficult parameter to determine (Cacciari and Futai, 2015), due to the fact that, fracture traces often have one or both ends censored in the outcrop. In this study, the circular scanline approach proposed by Rohrbaugh et al (2002) was used to determine the mean trace lengths for Site 1 and 2. The approach was used, not only to eliminate orientation bias observed in rectangular window sampling, but also to reduce time spent on data collection.

4.0 Results and Discussions

4.1 Computed Fracture Sets and Properties for Site 1

4.1.1 Orientation and Fracture Sets.

Fracture planes generally do not occur with random orientations, but belong to different fracture sets. Based on stereonets of the poles to planes of fracture orientations (Figures 5) for the fracture data for Site 1, major and minor fracture sets can be identified for the different fracture types, joints and foliation planes for the various rock types. Two dominant directions, one ENE, and the second NE, and two minor sets, nearly N-S and WN striking fractures, can be identified from Rose diagram for combined data for Site 1 (Figure 5B)

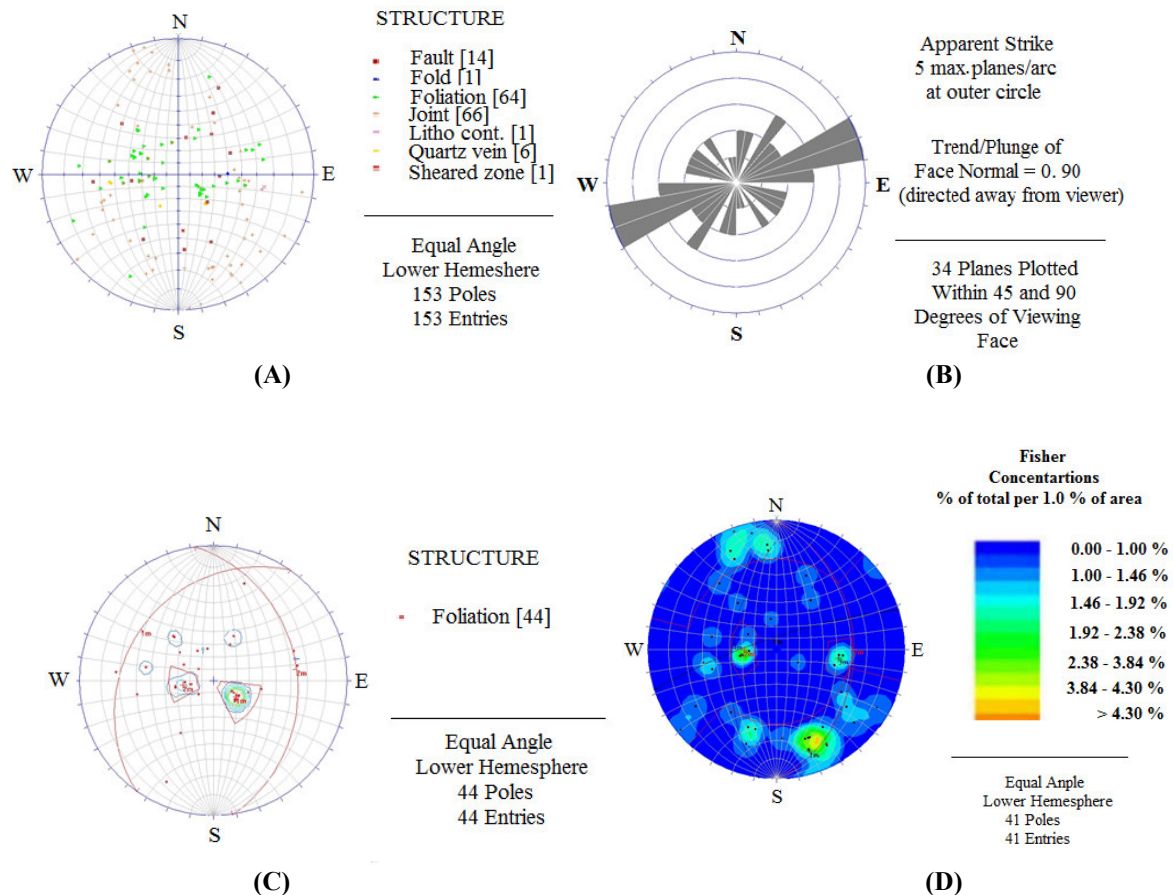


Figure 4 Equal Area Stereographic Projections of Structural Features Identified from Site 1, within the TSU. (A) Stereogram of Poles to Foliation (S₁), Faults, Joints Quartz Veins and Lithological Contacts for Site 1, (B) Rose Diagram for Combined Data for Site 1, (C) Foliation (S₁) in Quartzites, (D) Joints in Quartzites

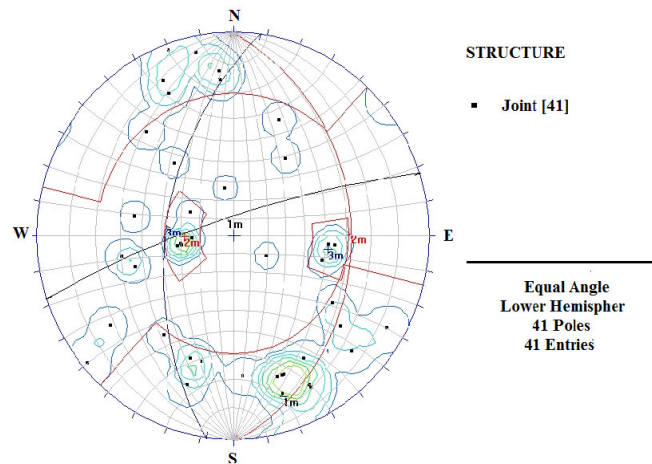


Figure 5 Contours of Lower-hemisphere Equal-area Projection of Joints Quartzites of Site 1, also showing Major Joint Sets

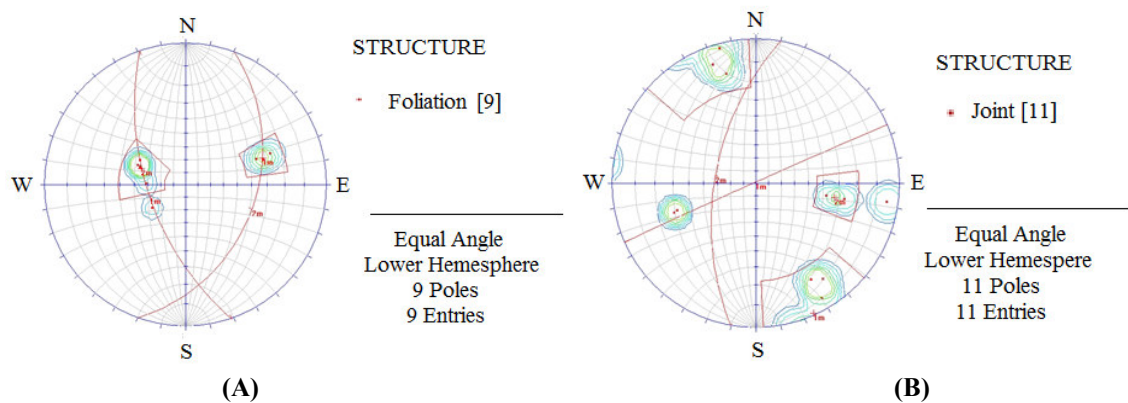


Figure 6 Contours of Lower-hemisphere Equal-area Projection of Fracture Types in Phyllites of Site 1. (A) Foliation and Major Foliation Sets, (B) Joints and Joint Sets

Joints and foliations are the most common fracture types at Site 1. From stereographic plots, it can be shown that, at least two sets of fractures occur for both joints and foliation planes in all the rock types. Table 2 present the mean orientations of fracture sets identified for Site 1.

Table 2 Summary of Characteristics of Fracture Sets Identified at Site 1 (TSU)

Rock type	Feature	Set	Orient. Dip/Dip direc./ Strike in (°)	Percentage in rock type (%)
Quartzite	Bedding	?		
	Foliation	Foliation set 1	23/305/125	65
		Foliation set 2	26/082/262	35
	Joints	Joint set 1	79/342/162	58
		Joint set 2	28/089/269	35
		Joint set 3	52/278/098	7
Fault	Fault set 1	46/209	100	
Phyllite/Quartzite intercalation	Bedding	?		
	Foliation	Foliation set 1	60/251/071	68
		Foliation set 2	37/110/290	32
	Joints	Joint set 1	89/336/249	72
		Joint set 2	58/280/173	21
Joint set 3		53/285/105	7	
Schist	Bedding	?		
	Foliation	?		
	Joints	Joint set 1	73/017/197	100

Joints within the quartzites of Site 1 indicates three fracture populations: two major populations (58% and 35%) and a minor one (7%). The most dominant joint set is steeply dipping (>75°). They are probably columnar joints. Foliation planes at Site 1 generally dip gently (< 30°). The joints do not appear to change their direction with the dip and strike of foliation planes and bedding in the quartzites, an indication they could be of younger generation. They seem to be closely related to the northeast-trending regional folds as reported by De Sitter (1956). From rose diagram of combine dataset (Figure 5a), fractures at Site 1 generally trend east-northeast (060-080), north-northeast (010-020°) (12%), and east-southeast (100-110°).

4.1.2 Fracture Frequency, Spacing and Spacing Distribution

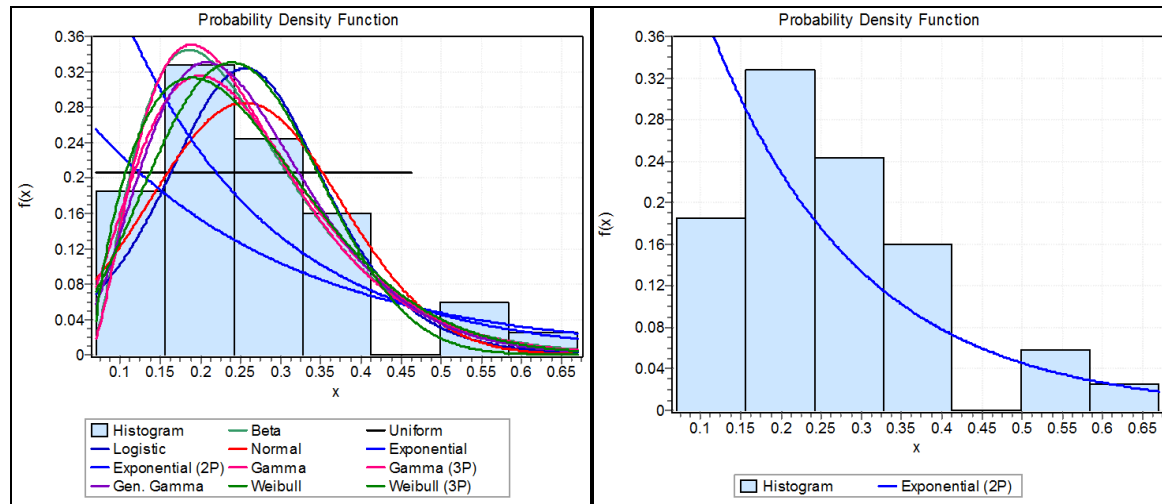
An analysis of fracture spacing data was carried out to determine the fracture total spacing distribution for the study site. The possible distribution forms and best fit model for Site 1 is shown in Figures 7 and the results of statistical analysis are summarised in Tables 5.5.

Distribution forms for both Site 1 indicated negative exponential distribution, which is in agreement with Priest and Hudson (1976), Wallis and King (1980) for most fracture spacing analysis. The distribution is a negative 2-parameter exponential function. The 2-parameter exponential probability density function (pdf) is given by:

$$f(x) = \lambda e^{-\lambda(x - \gamma)}, \text{ for } f(x) \geq 0, \lambda > 0, x \geq 0 \text{ or } \gamma \dots \dots \dots (1)$$

where, λ is the frequency or fracture per unit length.

The value of λ was determined as 5.3895 fracture/m, and γ as 0.07.



(A) **(B)**
Figure 7 Histogram and Total Fracture Distribution for Ablekuma linear Scanline Mapping: (A) Possible Distribution Models, (B) Best Fit Distribution Model is a Negative 2-parameter Exponential Function

The linear fracture frequency, mean fracture spacing, fracture density and intensity measured linearly along the scanline is presented in Table 3. The mean linear density indicates a close level of fracturing (>4 fractures/m) for the study site.

Table 3 Summary of Fracture Characteristics from Site 1

Fracture parameter	Value
Total scanline length (m)	238.0
Total number of surveyed fractures (N) from linear scanline	1128
Mean spacing (m)	0.256
Min. (m)	0.07
Max. (m)	0.67
SD for spacing	0.12
COV, spacing	0.47
Linear frequency (λ) (frac/m)	5.390
Mean trace length (l_m)	2.589
Areal density (ρ) (Frac/m ²)	5.57
Intensity (I)	13.18

4.1.3 Linear Intensity and Areal Intensity or Density

The linear fracture intensity (P_{10}) for Site 1 was computed as 4.739 fractures/m from 1128 fractures along 238.0 m scanline length. Areal fracture intensity (I_a) for Site 1 is 13.18 m (Table 4).

4.1.4 Fracture Mean Trace Length

Overall mean trace length for Site 1 and 2, determined from circular scanline survey data was 2.589 m (Table 4).

Table 4 Summary Statistics of Circular Scanlines and Mean Trace Lengths from Site 1

Circular Scanline ID	Parameter				
	n	m	Density (ρ)	Mean length (l_m) m	Intensity (I) $n/4r$ (m)
CSLAB001	51	25	3.98	3.203	12.75
CSLAB002	39	19	3.03	3.223	9.75
CSLAB003	34	25	3.98	2.135	8.50
CSLAB004	35	17	2.71	3.232	8.75
CSLAB005	38	25	3.98	2.386	9.50
CSLAB006	55	30	4.78	2.878	13.75
CSLAB007	60	47	7.48	2.004	15.00
CSLAB008	86	89	14.17	1.517	21.50
CSLAB009	91	68	10.82	2.101	22.75
CSLAB010	56	41	6.52	2.144	14.00
CSLAB011	31	11	1.75	4.425	7.75
CSLAB012	15	22	3.50	1.070	3.75
CSLAB013	72	48	7.64	2.355	18.00
CSLAB014	75	39	6.21	2.569	18.75
		Overall	5.57	2.589	13.18

r is the radius of the circular scanline, l is fracture trace length, n and m are the number of intersections with a circular scanline and the number of endpoints in a circular window enclosed by the circular scanline.

4.1.5 Qualitative Analysis of Fracture Data.

Figures 8 and 9 are plots for fracture trace length cumulative frequency, and aperture fracture length relation for Site 1.

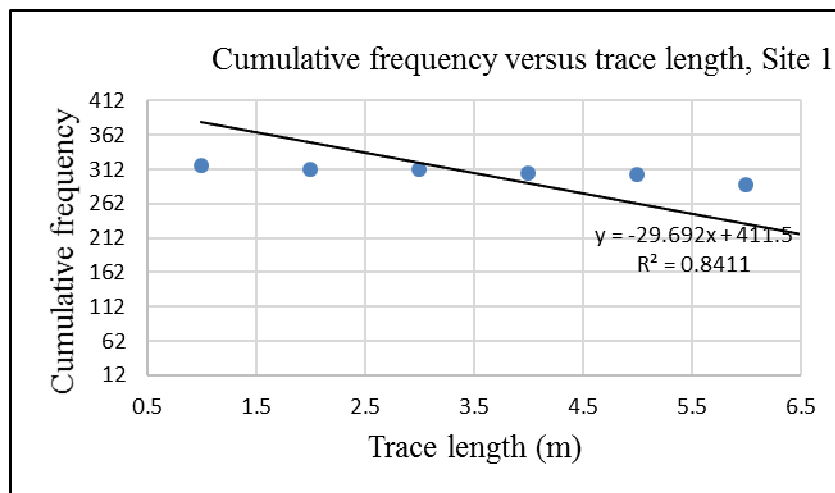


Figure 8 Linear Plot of Cumulative Versus Trace Length, Site 1

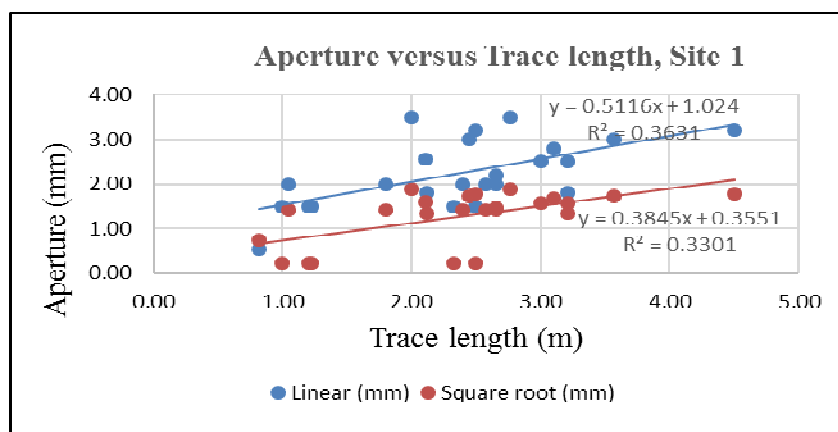


Figure 9 Trendlines for Linear and Square Root of Aperture Values versus Trace Length

Table 5 presents summaries of fracture parameters for the most dominant fracture sets at Site 1. The relationship between aperture and trace length is presented in Equation 2. The value of the coefficient of determination (R^2) suggests that there is a moderate relationship (over 35%) between fracture trace length and aperture from Site I data.

$$\text{Linear: } y = 0.5116x + 0.3551, \quad \dots \quad \dots \quad \dots \quad \dots \quad \dots \quad \dots \quad (2)$$

$$R^2 = 0.3631$$

Table 5 Summary of Fracture Parameters for Site 1

Parameter	Set 1	Set 2	Set 3
Orientation*	23/305/125	79/342/162	28/089/269
Length distribution (not height)	Negative exponential	Negative exponential	Negative exponential
Trace length (m)	Mean 5.50	Mean 2.60	Mean 2.85
	Min. trace length 0.65 m		
	Maximum trace length 6.32 m		
Aspect ratio (height: length)	0.32	0.30	0.35
Linear intensity (P_{10})	2.00	5.390	3.50
Volumetric intensity (P_{32})	??	??	??
Mean Aperture Width (mm)	Linear 2.233 mm		
	Square root 1.264 mm		
Aperture distribution	Linear	Linear	Linear
Aperture-length relationship,	Linear: $y = 0.5116x + 0.3551, R^2 = 0.3631$		
	Square root: $y = 0.3845x + 0.3551, R^2 = 0.3301$		

*Orientation is Expressed in. Dip/Dip Direction/Strike (°)

4.1.6 Geologic Controls on Fracturing

An analysis of the raw outcrop fracture data for Site 1 suggest little variation in fracture properties (orientation, trace length, intensity, aperture etc.) between the main rock units (quartzites and phyllites).

Plots of fracture orientation from one location to another indicate slight variation in fracture orientation probably as a result of folding.

Fracture spacing along individual scanlines show variable fracture linear intensity at Site 1, and probably across the TSU. Fracture properties appear to be subject to a number different geological controls. These include host lithology, stratigraphic thickness of the rock formation, fracture age and the presence of ductile or brittle deformation zones.

4.2 Computed Fracture Sets and Properties for Site 2, Danfa Area

4.2.1 Orientation and Fracture Sets.

As at Site 1, joints and foliations are the most common fracture types at Site 2. There is also a number of quartz veins at Site 2. From stereographic plots (Figure 10), it can be shown that a major and minor foliation strikes exist at Site 2. At least two sets of fractures occur for both joints and foliation planes in the rocks.

Dips of fractures within the acidic and basic gneisses were very variable as shown in rose diagram (Figure 5.10 (B)). Fracture sets were characterised mainly according to their trends. The dominant strike of the foliation is north-northeast (015-039°) dipping gently (35-40°) to the southeast. Two major joints sets were identified. The dominant set striking 290°, and dipping steeply (85°) southeast, while the subordinate set, dipping moderately (58°) southeast and striking 260°. Most fracture dips are sub-perpendicular to foliation planes. Fracture sets were characterised mainly according to their trends. Most joints within the gneisses are filled and sealed with quartz and other minerals (e.g. hematite, limonite, etc.). Table 6 presents a summary statistics of fracture sets identified for Site 2.

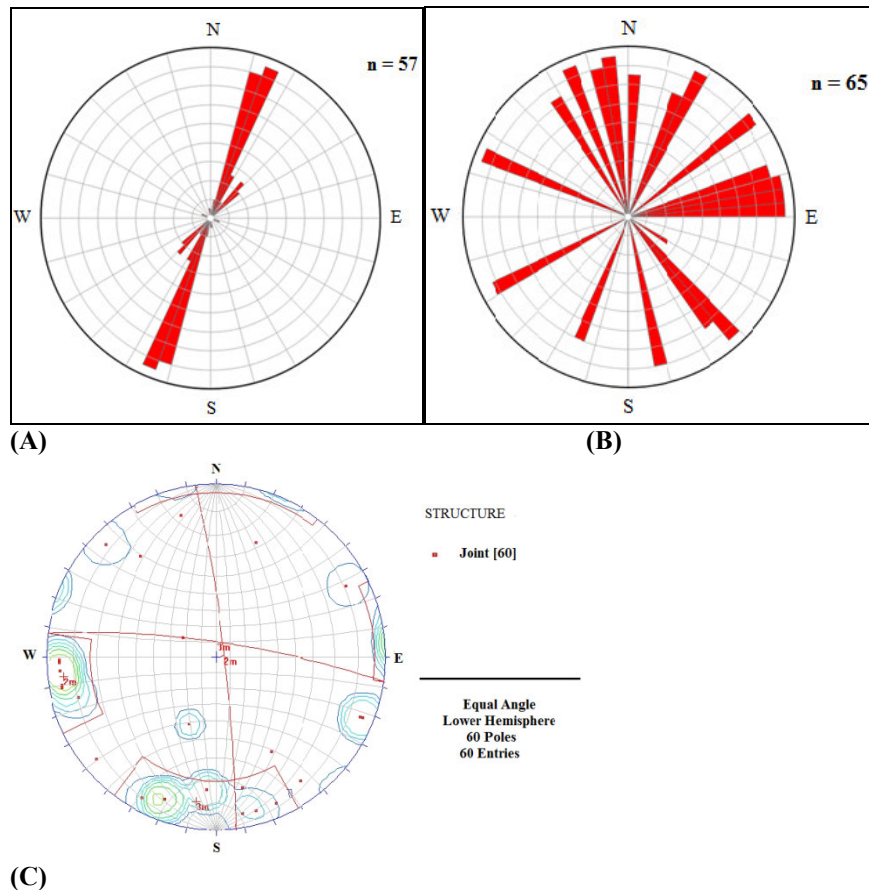


Figure 10 Stereographic Plots of Structural Features at Site 2 (Danfa area). (A) Plot of Rose Diagram of Strike of Foliation (S₁) at the Site, (B) Rose Diagram for Dips of Joints at Site 2 (C) Strikes of Joints

Table 6 Summary of Characteristics of Fracture Sets Identified at Site 2 (within Dahomeyan Formation)

Rock type	Feature	Set	Orientation in Dip/Dip direc. /Strike (°)	Percentage of data (%)
Acid gneiss	Foliation	Foliation set 1	40/075/346	80
		Foliation set 2	30/105//015	20
	Joints	Joint set 1	79/002/091	95
		Joint set 2	28/182/081	5
Basic gneiss	Foliation	Foliation set 1?	40/110/015	95
		Foliation set 2	35/288/030	5
	Joints	Joint set 1	85/200/290	80
		Joint set 2	58/170/260	18

4.2.2 Fracture Frequency, Spacing and Spacing Distribution

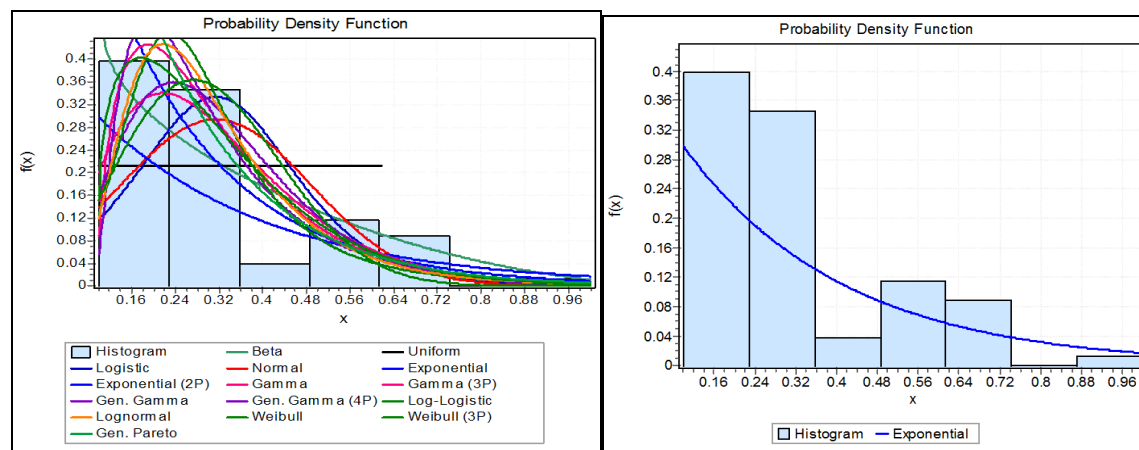
The best fit form of distribution model for the raw fracture spacing values for Site 2 was negative exponential probability distribution function (Figure 11), expressed mathematically as:

$$f(x) = \lambda e^{-\lambda x} \quad \dots \quad (3)$$

where, $f(x)$ is the frequency of fracture spacing x , and λ is the average number of fractures per metre. This is a

one parameter (λ) distribution with the mean and standard deviation (SD), both equal to $\frac{1}{\lambda}$. λ was determined as 3.1811.

The overall mean fracture spacing for Site 2 was 0.314 m.



(A) (B)
Figure 11 Histogram and Total Fracture Distribution for Danfa Linear Scanline Mapping: (A) Possible Distribution Models, (B) Best Fit Distribution Model is Negative Exponential Probability Function

The linear fracture frequency, mean fracture spacing, fracture density and intensity measured linearly along the scanline is presented in Table 6. The mean linear density indicates a close level of fracturing (>4 fractures/m) for the site. Maximum spacing was 1.0 m.

Table 6 Summary of Fracture Characteristics from Site 2.

Fracture parameter	Value
Total scanline length (m)	156.0
Total number of surveyed fractures (N) from linear scanline	629
Mean spacing (m)	0.314
Min. (m)	0.10
Max. (m)	1.00
SD for spacing	0.18
COV, spacing	0.58
Linear frequency (λ) (frac/m)	3.181
Mean trace length (l_m)	2.881
Areal density (ρ) (Frac/m ²)	3.57
Intensity (I)	9.50

4.2.3 Linear Intensity and Areal Intensity or Density

The linear fracture intensity (P_{10}) for Site 2 was computed as 4.030 fractures/m from 629 fractures along 156.0 m scanline length. Areal fracture intensity (I_a) for Site 2 was 9.50 m (Table 5.10).

4.2.4 Fracture Mean Trace Length

Overall mean trace length for Site 2, determined from circular scanline survey data was 2.881 m (Table 7).

Table 7 Summary Statistics of Circular Scanlines and Mean Trace Lengths from Site 2

Circular Scanline ID	Parameter				
	n	m	Density (ρ)	Mean length (l_m) m	Intensity (I) $n/4r$ (m)
CSLDA001	24	22	3.50	1.714	6.00
CSLDA002	38	18	2.87	3.314	9.50
CSLDA003	42	25	3.98	2.536	10.50
CSLDA004	40	11	1.75	5.709	10.00
CSLDA005	49	26	4.14	2.959	12.25
CSLDA006	45	30	4.78	2.355	11.25
CSLDA007	43	26	4.14	2.577	10.75
CSLDA008	48	32	5.10	2.355	12.00
CSLDA009	49	38	6.05	2.024	12.25
CSLDA010	35	16	2.55	3.434	8.75
CSLDA011	22	19	3.03	1.818	5.50
CSLDA012	29	13	2.07	3.502	7.25
CSLDA013	30	15	2.39	3.140	7.50
		Overall	3.57	2.881	9.50

r is the radius of the circular scanline, l is fracture trace length, n and m are the number of intersections with a circular scanline and the number of endpoints in a circular window enclosed by the circular scanline.

4.2.5 Qualitative Analysis of Fracture Data

Figure 11 is plot of aperture: fracture trace length relation for Site 2.

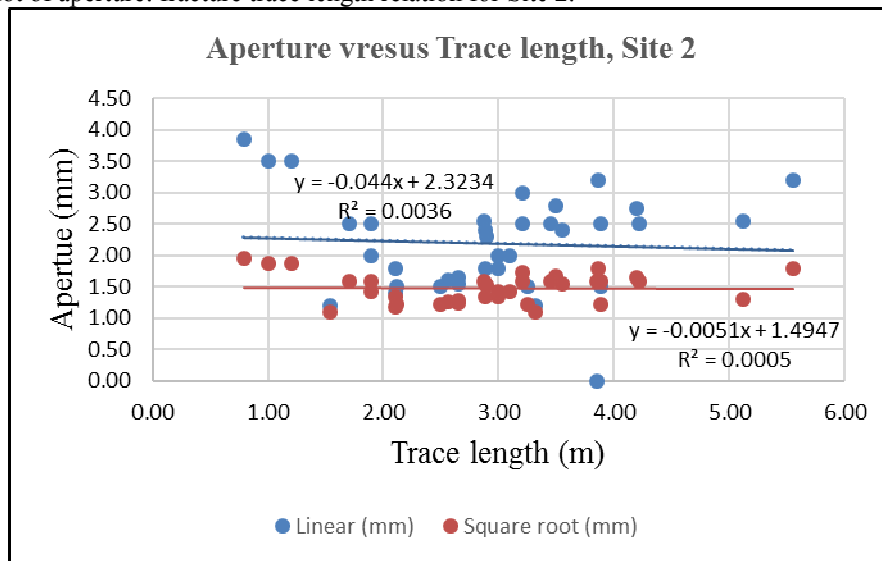


Figure 11 Aperture: Trace Length Relation, Site 2

Table 8 are summaries of fracture parameters for the most dominant fracture sets at Site 2. The relationship between aperture and trace length is presented in Equations 5.4. The value of the coefficient of determination suggests that there is a moderate relationship (<1%) between fracture trace length and aperture from Site 2 data.

$$y = -0.0044x + 2.3234 \quad \dots \quad R^2 = 0.0036 \quad (5.4)$$

Table 8 Summary of Fracture Parameters for Study Site 2

	Set 1	Set 2	Set 3
Orientation*	40/110/015	85/200/290	58/170/260
Length distribution (not height)	Normal	Normal	Normal
Trace length (m)	Mean 6.50	Mean 3.00	Mean 2.90
	Min. 0.79		
	Max. 6.45		
Aspect ratio (height: length)	0.2	0.25	0.25
Linear intensity (P ₁₀)	3.00	3.50	2.50
Volumetric intensity (P ₃₂)	-	-	-
Mean Aperture Width (m)	Linear: 2.2639 mm		
	Square root: 1.4798 mm		
Aperture distribution	Linear	Linear	Linear
Aperture-length relationship	Linear: $y = -0.0044x + 2.3234, R^2 = 0.0036$		
	Square root: $y = -0.0051x + 1.4947, R^2 = 0.0005$		

*Orientation is Expressed in. Dip/Dip Direction/Strike (°)

4.2.6 Geologic Controls on Fracturing

Fracture sets at Site 2 appear to be more homogenous. Joints angles at this site are variable, while plots of their strikes indicate two sets.

3.2.3 Comparison of Fracture Characteristics for Site 1 and Site 2

Table 9 presents the comparison of the computed fracture characteristics from Site I and Site 2. Fracture spacing distribution for Site 1 showed a negative 2-parameter exponential function, while, that of Site 2 was simply a negative exponential probability density function (pdf). A negative exponential distribution of fracture spacing values appear to be a good approximation to the true distribution patterns (Priest and Hudson, 1976). Site 2 was simply a negative exponential probability density function (pdf), probably as a result of data compiled from a small number of measurements (sampling error).

Comparing the values of fracture intensity, mean trace lengths, and fracture spacing from the two sites, it is clear fracturing is more intense at Site 1 within the TSU than Site 2 in the Dahomeyan Formation.

Table 9 Summary of Fracture Characteristics from Site 1 and Site 2

Fracture parameter	Study site	
	Site 1 (TSU)	Site 2 (Dahomeyan Formation).
Total scanline length (m)	238.0	156.0
Total number of surveyed fractures (N) from linear scanl.	1128	629
Mean spacing (m)	0.256	0.314
Min. (m)	0.07	0.10
Max. (m)	0.67	1.00
SD for spacing	0.12	0.18
COV, spacing	0.47	0.58
Linear frequency (λ) (frac/m)	5.390	3.181
Mean trace length (lm)	2.589	2.881
Areal density (ρ) (Frac/m ²)	5.57	3.57
Intensity (I)	13.18	9.50

Comparing the means of fracture spacing for both Site 1 (TSU) and Site 2 (Dahomeyan formation) with ISRM (1978)

Conclusions

The following conclusions can be drawn from the objectives of the study:

- ❖ The integrated methods approach of structural geological mapping, linear and circular survey methods are applicable to fracture data sampling, and provided adequate information for identifying major and minor fracture sets and their orientations from outcrops in the study area.
- ❖ Joints and foliations are the most common fracture types at both Site 1 and 2.
- ❖ The rocks observed at Site 1 in the TSU and Site in the DGC exhibit differences in joint fracture geometric and intrinsic properties, particularly infill material. Analysis of field data show that the gneisses of the DGC are more mechanically resistant and more rigid and have a higher cohesion than the quartzites and phyllites of the TSU. The quartzites and phyllites have been more intensely fractured than the gneisses, though, the two might have undergone the same tectonic history.
- ❖ Estimates of fracture spacing for the two study sites showed close to moderate fracture spacing. Fracture spacing distribution for Site 1 showed a negative 2-parameter exponential function, while, that of Site 2 was simply a negative exponential probability density function (pdf). A negative exponential distribution of fracture spacing values appear to be a good approximation to the true distribution patterns (Priest and Hudson, 1976). Site 2 was simply a negative exponential probability density function (pdf), probably as a result of data compiled from a small number of measurements (sampling error).
- ❖ Linear fracture density or intensity (P_{10}) from the 7 scanlines at Site 1 ranged from 3.50 fractures/m to 6.26 fractures/m, compared to fractures at Site 2, which have fracture linear density ranging from 2.34 fractures/m to 5.04 fractures/m.
- ❖ The mean linear fracture intensity for Site 1 was computed as 4.739 fractures/m and 4.030 fractures/m from 629 fractures along a total of scanline of 156.0 m for Site 2.

There appear to be a lithological and/or stratigraphic thickness control on fracture density, as fracturing was more intense in the medium grained less thick quartzite beds of the Site 1, within TSU compared to the coarse grain much thicker stratigraphic units of gneiss of Site 2 within the DF. The general trend of combined fracture orientation data for the Study area (Accra-Tema), appear to conform to the general northeast–southwest structural pattern of southeast Ghana.

References

- Affaton, P., (1990). In: Le Bassin des Volta (Afrique de l'Ouest): une Marge Passive d'age Proteozoïque Supérieur, Tectonise e au Panafricain (600 ± 50 Ma). ORS- TOM, Paris, pp. 500. Collection Etudes et Theses.
- Affaton, P., Rahaman, M. A., Trompette, R., and Sougy, J., (1991). The Dahomeyide orogen: tectonothermal evolution and relationships with the Volta basin. In: Dallmayer, Le corche (Eds.), The West-African Orogen and Circum Atlantic Correlatives. Projet 233. ICGP, IUGS, UNESCO, pp. 107-122.
- Akpan, O., Nyblade, A., Okereke, C., Oden, M. Emry, E. and Julià, J. (2016) Crustal structure of Nigeria and Southern Ghana, West Africa from P-wave receiver functions. Tectonophysics
- Anon (1997) Consultancy for the study of the ATMA development and Investment programme and of the Rehabilitation/Replacement of Kpong-Tema-Accra water pipeline, pp. 4–21.
- Blay, P. K. (1982) Geology of 1/4 Field Sheets 184, 185 and 187. Ghana Geological Survey Bulletin, 45.
- Boadu, F. K., and Long, L. T. (1996), Effects of fractures on seismic-wave velocity and attenuation. Geophys. J.

- Int., 127, pp. 86-110.
- Brace, W. F. (1980). Permeability of crystalline and argillaceous rocks, *Int. J. Rock. Mech. Min. Sci. Geomech. Abstr.* 17, 241-251.
- Brown, S. R., and Scholz, C. H. (1986). Closure of rock joints, *J. Geophys. Res.*, 91, 4939-4948.
- Brown, S. R. (1989). Transport of fluid and electric current through a single fracture, *J. Geophys. Res.*, 94, 9429-9438.
- Caby, R. (1989) Precambrian terrains of Benin-Nigerian and Northeast Brazil and Late Proterozoic South Atlantic rift. *Geol. Soc. American Spec. Paper*, 230, 145-158.
- Dickson, K. B., and Benneh, G. (1988). *A New Geography of Ghana*, Longman Group (FE) Ltd, 170 p.
- Einstein, H. H., and Baecher, G. B. (1983), Probabilistic and statistical methods in engineering geology: *Rock Mechanics and Rock Engineering*, Vol. 16, p. 39-72.
- Fisher, N. I. (1993), *Statistical Analysis of circular data*, Cambridge, New York, 277 p.
- Goodman, R. E. (1976). *Methods of Geological Engineering*, West Publishing, St. Paul, MN.
- GSD (1988), *Geological Map of Ghana (1:1 000 000) with mineral deposits*. Geological Survey Department of Ghana, Accra.
- Hoek, E. and Bray, J. W. (1981), *Rock Slope Engineering*. Revised Third Edition, The Ints of Mining and Metallurgy, London, 358pp.
- Hudson, J. A. and Harrison, J. P. (1997), *Engineering rock Mechanics: An introduction to the principles*. Published by Elsevier Science Ltd. 444pp.
- Junner, N. R., Bates, D. A., Tillotson, E., and Deakin, C. S. (1939) "The Accra Earthquake of 22nd June, 1939," *Gold Coast Geological Survey Bulletin*, No. 13, 1941, pp. 1-57.
- Junner, N. R. (1941). The Accra Earthquake of 1939. *Bulletin* 13, Gold Coast Geological Survey, 67 p.
- Kesse, G. O. (1985). The mineral and rock resources of Ghana, Balkema, Rotterdam, 32-41.
- Leary, P. C. Crampin, S. and McEvilly, T. V. (1990). Seismic Fracture Anisotropy in the Earth's Crust: An Overview. *Jour. of Geophy. Res.*, Vol. 95, No. B7. pp 11105-11114.
- Mahaman, S. T., Affaton, P. Anum, S., and Fleury, T. J. (2012), Pan-African Paleostresses and Reactivation of the Eburnean Basement Complex in Southeast Ghana (West Africa). *Journal of Geological Research* Volume 2012, Article ID 938927, 15 pages doi:10.1155/2012/938927
- Mani, R. (1978). The geology of the Dahomeyan of Ghana. *Geology of Ghana Project*. Ghana Geological Survey Bulletin, 45p.
- Mauldon, M., Dunne, W.M., Rohrbaugh Jr., M. B., (2001). Circular scanlines and circular windows: new tools for characterizing the geometry of fracture traces. *Journal of Structural Geology* 23, 247-258, <http://dx.doi.org/10.1016/S0191->
- McCallien, W. J. (1962) "The Rocks of Accra," University of Ghana Publ. Board, Legon.
- Muff, R., and Efa, E., (2006) Explanatory notes for the coastal stability map 1: 100,000 for Greater Accra Metropolitan Area, 18p.
- Murphy, H., Huang, C., Dash, Z., Zyvoloski, G., White, A., (2004), Semi-analytical solutions for fluid flow in rock joints with pressure-dependent openings. *Water Resour. Res.* 40, W12506, <http://dx.doi.org/10.1029/2004WR003005>.
- Nude, P. M., Shervais, J., Attoh, K., Vetter, S. K., and Barton, C., (2009) Petrology and geochemistry of nepheline syenite and related carbonate-rich rocks in the Pan- African Dahomeyide orogen, southeastern Ghana, West Africa. *Journal of African Earth Sciences*, 55, 147-157.
- Olson, J. E., Laubach, S. E. and Lander, R. H. (2009), Natural fracture characterization in tight gas sandstones: Integration mechanics and diagenesis: *AAPG Bulletin*, Vol. 93, pp. 1535-1549.
- Pahl, P. J. (1981), Estimating the mean length of discontinuity traces: *International Journal of Rock Mechanics and Mining Sciences and Geomechanics Abstracts*, Vol. 18, pp. 221-228.
- Peacock, D. C. P., Knipe, R. J., Sanderson, D. J. (2000), Glossary of normal faults. *Journal of Structural Geology* 22, pp. 291-305.
- Priest, S. D., (1993), *Discontinuity analysis for rock engineering*: London, United Kingdom, Chapman & Hall, 473 p
- Rohrbaugh Jr, M. B., Dunne, W. M., Mauldon, M., (2002), Estimating fracture trace intensity, density and mean length using circular scanlines and windows. *AAPG Bulletin* 86, 2089-2104, <http://dx.doi.org/10.1306/61EEDE0E-173E-11D7-8645-000102C1865D>.
- Rohrbaugh Jr., M. B., Dunne, W. M., Mauldon, M., (2002). Estimating fracture trace intensity, density and mean length using circular scanlines and windows. *AAPG Bulletin* 86, 2089-2104, <http://dx.doi.org/10.1306/61EEDE0E-173E-11D7-8645-000102C1865D>.
- San, M. (2009). The Stochastic assessment of strength and deformability characteristics for appropriate apyrochastic rockmass. *Int. J. Rock., Min. Sci.* 46(3), 613-628.
- Schittkowski, K. (EASY-FIT 2002): A software system for data fitting in dynamic systems. *Struct Multidisc*

- Optim., 23, pp. 152-169. Springer-Verlag
- Van der Pluijm, B. and Stephen Marshak, S (2004). Earth Structure: An Introduction to Structural Geology and Tectonics (Second Edition), WW Norton & Company
- Warpinski, N. R. (1991): Hydraulic fracturing in tight, fissured media, SPE 20154, J. Petroleum Technology, 43:2, pp. 146-209.